PHYSICAL REVIEW B VOLUME 54, NUMBER 6 1 AUGUST 1996-II

Magnetic properties, relaxation, and quantum tunneling in $CoFe_2O_4$ nanoparticles embedded in potassium silicate

X. X. Zhang,* J. M. Hernandez, and J. Tejada
Departament de Fisíca Fonamental, Universidad de Barcelona, Diagonal 647, 08028 Barcelona, Spain

R. F. Ziolo
Wilson Center for Research and Technology, Xerox Corporation, Webster, New York 14580

(Received 1 March 1996)

We report magnetic properties and magnetic relaxation phenomena in a sample comprised of nanocrystalline $CoFe_2O_4$ (~97%)+γ-Fe_2O_3 (~3%) and polymer in potassium silicate (as magnetic glass) nanoparticle systems in which two very different barrier distributions contributed to the relaxation behavior. We have demonstrated experimentally that only energy barrier distributions and the thermal activation process could not account for a plateau in the viscosity data at low temperatures. Quantum tunneling of magnetization is suggested below ~3 K. [S0163-1829(96)00329-3]

INTRODUCTION

It is well known that the magnetic behavior of a small particle depends on its relaxation time τ,

$$\tau = \tau_0 \exp\left(\frac{KV}{k_B T}\right), \tag{1}$$

where $\tau_0 = \Gamma_0^{-1}$, Γ_0 is the attempt frequency on the order of 10^9–10^{13} s^{-1}, k_B the Boltzmann constant, and T the temperature; K and V are, respectively, the anisotropy constant and volume of the particle. Considering a system consisting of identical, noninteracting single-domain particles embedded in a solid nonmagnetic matrix, when $k_B T \gg KV$, the relaxation time becomes small and the magnetization vector rotates quickly in response to a change of applied field or temperature. The superparamagnetic thermal equilibrium can be reached in a very short time (~10^{-6} s). With a typical measuring time of equipment, t_{mes}~100 s, the measured magnetization curves versus temperature and applied field can be described very well by the Curie law and Langevin equation, respectively. For $KV \gg k_B T$, τ can be very large and the thermal dynamic equilibrium state is very difficult to observe, since the barriers arising from the anisotropy obstruct the magnetization vector from rotating to a lower-energy state. This case is generally called the blocked state. In the presence of size distribution, the response to an applied field of the magnetization can be divided into two steps: In the first step, the magnetization decays within the metastable states, and also due to the decay of metastable states in the smallest particles. The system of particles then enters the stage in which the relaxation is due to particles whose metastable states have a lifetime corresponding to the running time of the measurement. This can be due to either thermal activation or quantum tunneling.[1]

The magnetic relaxation measurement is a useful tool which helps to get a deeper understanding of the dynamic behavior of the magnetization vector of small particles. In the last years, it has also been demonstrated that quantum tunneling of the magnetization in magnetic materials and quantum tunneling of vortices in superconductors can be more directly observed with magnetic relaxation measurements.[1–5]

When a magnetic field, orienting the moments of identical particles, is removed, the time dependence of the magnetic moment of the system is governed by the exponential relaxation law

$$M = M_0 \exp(-\Gamma t) \tag{2}$$

where $\Gamma = \Gamma_0 \exp(-U/k_B T) = \Gamma_0 \exp(-KV/k_B T)$. For the thermally activated process, when T goes to zero, so does Γ. If one finds $\Gamma(T) = \text{const}$, a temperature-independent relaxation rate below a certain temperature T_C, the relaxation process should be attributed to quantum tunneling. To our knowledge, exponential quantum relaxation has only been observed in a $TbFeO_3$ single crystal[6] and tetragonal crystals of Mn_{12} acetate complex.[7,8]

In practice, however, it is difficult to have a system of identical barriers. The real system generally has a distribution of size, anisotropy, and shape of the particles which leads to a barrier distribution $f(U)$. For a system having a broad barrier distribution, the magnetization relaxation, at $T < T_B$, can be described by the logarithmic law[1]

$$M = M(t_0)[1 - S \ln(t/t_0)],$$
$$S = \frac{k_B T}{\langle U \rangle}. \tag{3}$$

Here S is the magnetic viscosity, t_0 is an arbitrary time after changing the field, $\langle U \rangle$ is the average energy barrier, and T_B is the blocking temperature which is generally measured in the zero-field-cooled magnetization process. At the thermally activated regime, $T_C \leqslant T \ll T_B$, S is proportional to T, and at the quantum-tunneling-dominated regime $T \leqslant T_C$, $S = \text{const}$, where T_C is the crossover temperature. Thus the relaxation is a useful method to observe the quantum tunneling of magnetization (QTM) effect, which is not limited by the character of the materials.

One argument on the behavior of viscosity is that the plateau in low temperatures could be due to the singular energy distribution at low temperatures.[9] This argument is based on the calculation and needs experimental examination.

In this paper, we report a systematic study of magnetic properties of $CoFe_2O_4$ nanoparticles, which has been embedded in a silicate matrix. This sample has two distributions of energy barriers; one is very broad at high temperatures and the other is very narrow at low temperatures. We will demonstrate that the small energy barrier does not cause a plateau in viscosity, but gives a temperature-dependent viscosity behavior. The contribution of a low-temperature energy barrier distribution to the relaxation can be eliminated by applying a large magnetic field.

EXPERIMENT

Sample preparation

Starting materials were prepared as described in Ref. 10. The material, which consists of nanocrystalline $CoFe_2O_4+\gamma$-Fe_2O_3 (particle diameter $\sim$3 nm) in polystyrene resin,[10] was then ground in water to form a stable aqueous colloid.[11] Then we mixed the aqueous colloid and potassium silicate 1:1, and heated it at 308 K for 1 h to have the solid glass sample.

Magnetic measurements

All magnetic measurements were performed with a commercial Quantum Design superconducting quantum interference device with low and high magnetic fields (up to 5 T) in the temperature range 1.8–320 K. In the low-field measurements, the so-called zero-field-cooled (ZFC) and field-cooled (FC) magnetizations were obtained by using the following procedure: first the sample was cooled from room temperature to a low temperature in zero applied field, after which a field $H=0.5$ kOe was applied; then the variation of magnetization with temperature (ZFC process) was measured in the temperature-increasing process until $T=320$ K. Second, the sample was cooled again, keeping the same applied field to the same low temperature; then the temperature was increased, and the variation of magnetization with temperature (FC process) was measured. By analyzing the ZFC-FC magnetization data we can get information about the blocking temperature and energy distribution, from which the average size and distribution of the particles can be estimated, assuming that the particles have the same anisotropy.

Another kind of magnetic characterization of the material is their dynamic magnetic behavior, which can be revealed by magnetic relaxation measurements. In order to perform the relaxation measurement, first the sample was FC cooled in an applied field $H_1(=4$ kOe) to a target temperature, after which the applied field was changed to $H_2(=-1, 4, -7,$ and -8 kOe), then the change of remnant magnetization with time was measured for a few hours. After this measurement, the sample was heated to higher temperature with applied field H_1 and cooled down to another target temperature for another relaxation measurement.

The dependence of magnetization on the applied field and the hysteresis loops were measured up to 5.5 T at different temperatures, by which we obtained the temperature dependence of the saturation magnetization M_S, coercive field H_C, and remnant magnetization Mr, as well as the switching field distribution.

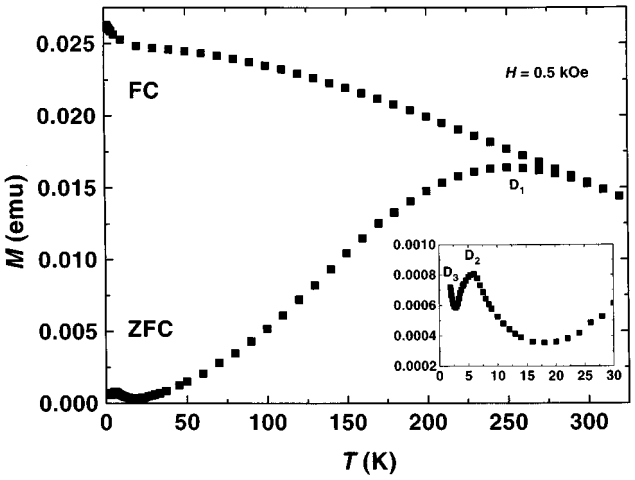

FIG. 1. Temperature dependence of the magnetization obtained in the ZFC-FC process with applied field $H=0.5$ kOe. Inset: the low-temperature range of the ZFC curve.

RESULT AND DISCUSSION

Figure 1 shows the temperature variation of magnetization in the ZFC-FC process with applied magnetic field $H=0.5$ kOe. The most remarkable feature in the ZFC curve is the two nonoverlapping peaks at temperatures around 6 and 250 K, respectively. Below 3 K, the magnetization increasing as temperature decreases could be due to another set of very small particles or only to the pure paramagnetic contribution. These peaks arise from the distribution of relaxation time or energy barrier distribution of the system. These energy distributions at different temperature ranges detected in the ZFC magnetization process may be due to the distribution of particle size, shape, and anisotropy constant. Here we call the two separated peaks distribution D_1 at 15 K$<T$, distribution D_2 at 3 K$<T<$15 K, and distribution D_3 below 3 K; see the inset in Fig. 2. The ratio of D_1 and D_2 can be estimated roughly as M_{ZFC} (6 K)/M_{ZFC} (250 K) $\sim$0.2%, although M_{ZFC} (6 K) receives a very small contribution from D_1, due to the fact that the particles in D_1 having a blocking temperature T_B around 250 K; thus their susceptibility should be very small in the blocked state, in an applied field much smaller than their anisotropy field. Here we do not consider the contribution of D_3, because, in a field of 0.5 kOe, the particles behave superparamagnetically, and will not contribute to the relaxation measurements with an applied field $H_2 \geqslant 0.5$ kOe. Most of the particles in D_2 were at the blocked state in an applied field $H=0.5$ kOe; see the ZFC curve in Fig. 1. When the applied field increased to 4 kOe, most of them behaved superparamagnetically (see the inset in Fig. 2) at applied magnetic field. In the ZFC process with an applied field, $H=6$ and 8 kOe, the peak due to D_2 almost disappeared, and the particles behaved superparamagnetically (Fig. 3) (this can be determined by the plot $1/\chi$ versus T). Thus if one applies a field $-H_2 \geqslant 6$ kOe in the

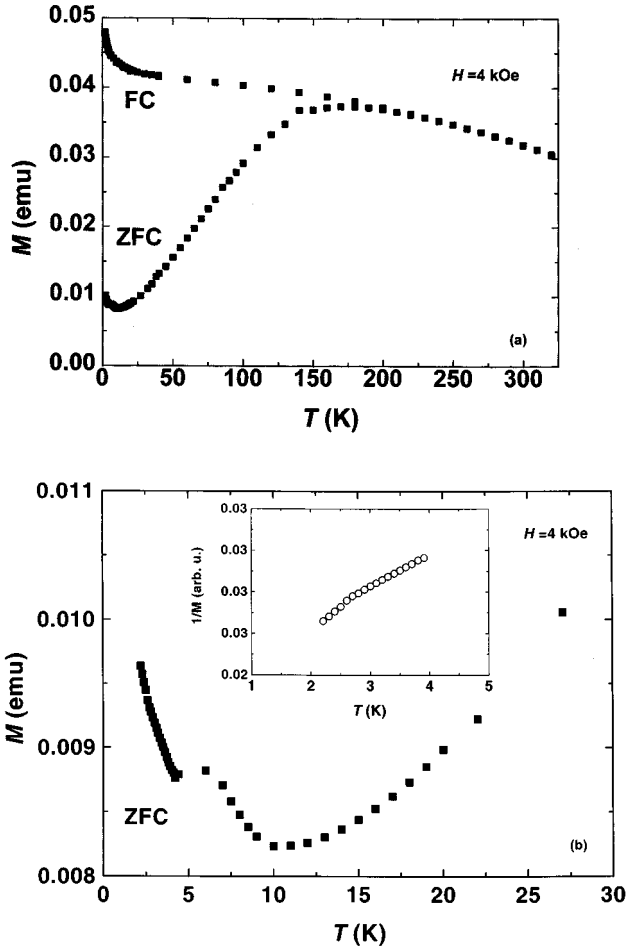

FIG. 2. (a) Temperature dependence of the magnetization obtained in the ZFC-FC process with applied field $H=4$ kOe. (b) Low-temperature range of the ZFC curve in (a). Inset: the $1/M$ vs temperature.

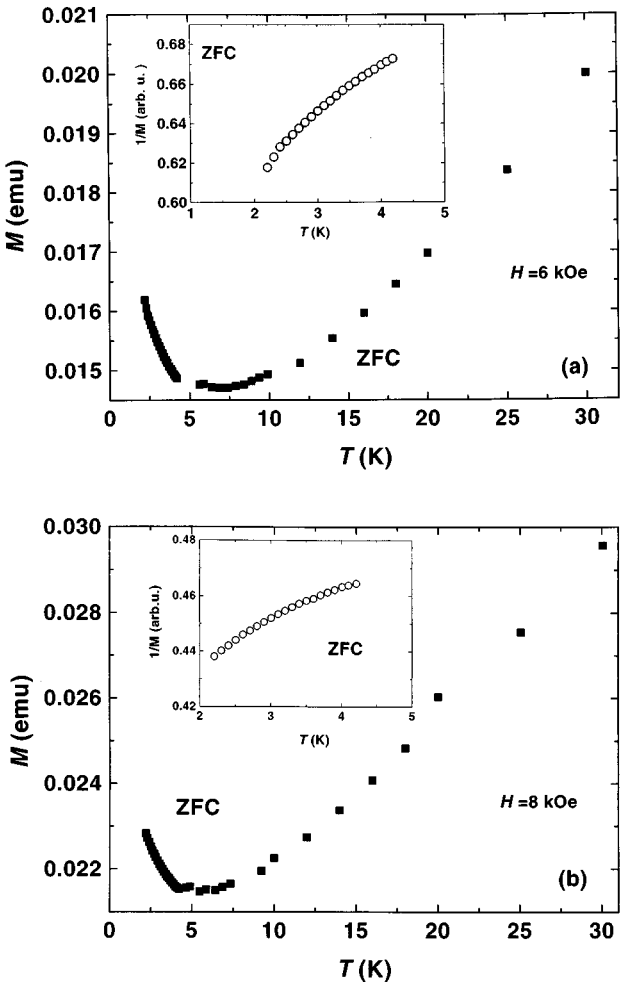

FIG. 3. Temperature dependence of the magnetization obtained in the ZFC-FC process with applied field in the low-temperature range: (a) $H=6$ kOe. (b) $H=8$ kOe. Insets: $1/M$ vs temperature for two applied fields.

relaxation measurements, the particles in D_2 will not contribute to long-time relaxation of the magnetization, because their magnetic moments immediately change to the H_2 direction, the thermal equilibrium state, when H_2 is applied.

In Fig. 4, we display the magnetization curves obtained at different temperatures, with applied magnetic fields varying between 0 and 55 kOe. At high temperatures of 100, 250, and 300 K, it appears that the magnetization saturates like any ordinary ferromagnet for fields in excess of 10 kOe. However, at lower temperatures of 10 and 2 K, the magnetization does not saturate, even at 55 kOe. The explanation for this behavior is that the sample can be considered as a two-magnetic-component system: (1) a ferromagnetic component considering all the particles that exceed the critical size for ferromagnetic behavior, in which (2) the particles are small enough to be considered as superparamagnetic or paramagnetic. Clearly the above classification depends on the temperature at which the magnetization curves were measured.

The difficulty of saturation at lower temperatures, for example, $T=2$ K, indicates that some small particles are still in the superparamagnetic state which corresponds to the ZFC-FC results ($T<3$ K). At higher temperatures, for example at 100 K, the magnetization was saturated at $H=20$ kOe, although the small particles are still in the superparamagnetic state, which can be explained due to the small quantity (or ratio) of the small particles, and, because of their inverse temperature dependence on the superparamagnetic susceptibility, the contribution of these particles to the total magnetization is too small to be detected.

Figure 5 shows parts of the hystereses obtained at different sample temperatures. One feature should be noted. The irreversible field at which the high branch of the magnetization, as the field decreases, and the lower branch of the magnetization, as the field increases, begin to separate, decreases with increasing temperature. This irreversible field can be considered as the minimum anisotropy field, H_K.[4] At $T=2$ and 10 K, $H_K\sim 5$ and 3 T, respectively. The switching field distribution dM/dH is also obtained from the hystereses data, and presented in Fig. 6.

In Fig. 7, we represent the dependence of the coercive field on the temperature; the inset is the plot of squareness $\mathrm{Sq}=Mr(H=0)/Ms(H=50\ \mathrm{kOe})$ changing with the temperature. The temperature dependence of H_C can be fitted by the $H_C(T)=H_C(1-\sqrt{T/T_B})$ for the small particles,[12] with $H_C(0)=\sim 11.3$ kOe. At the temperature range from 2 to 25 K, Sq$\sim$0.5, indicating that, for the applied field $H=0$, al-

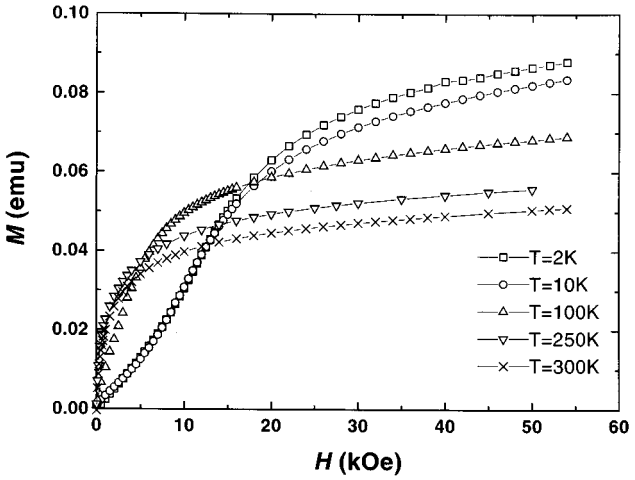

FIG. 4. Magnetization vs applied magnetic fields obtained at different sample temperatures.

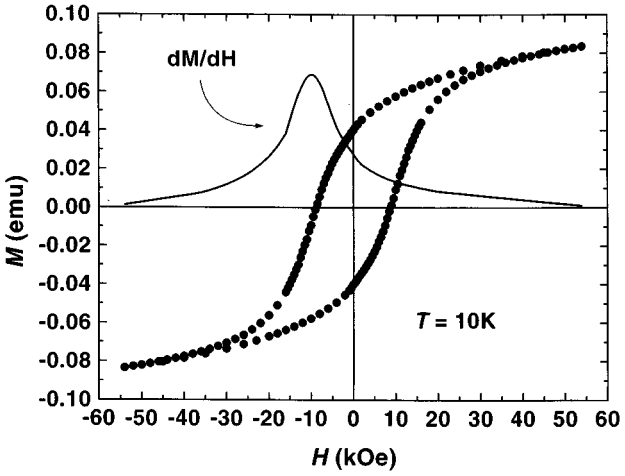

FIG. 6. Hysteresis loop obtained at temperature $T=10$ K, and the switching field distribution dM/dH.

most all the particles are at the blocked state.[13] With increasing temperature, the ratio of remnant magnetization to saturation decreases, which suggests that the particles begin to behave superparamagnetically, or that their relaxation time is less than the measuring time of 100 s.

In Fig. 8, we plot the magnetization versus logarithmic time obtained in the relaxation measurements, at different sample temperatures, with applied magnetic field $H_2=-8$ kOe, after the field cooled in a field $H_1=4$ kOe from high temperature of 300 K. The best fitting to the time dependence of the magnetization is the logarithmic time law [Eq. (3)]. One feature should be noted in Fig. 8(a): the remnant magnetization decreases as the temperature T goes to zero, which is contrary to what is observed in normal ferromagnetic materials. This phenomenon supports our analysis that with high applied field in relaxation measurements, the particles in D_2 do not contribute to long time relaxation. Their magnetic moments rotate immediately in response to the applied field H_2, which makes the remnant magnetization decrease with decreasing temperatures due to the superparamagnetic susceptibility which is inversely dependent on temperature. With the increasing temperature at which the relaxation was performed, the superparamagnetic contribution becomes less and less, and the remnant magnetization of the sample changes to the normal ferromagnetic behavior; see Fig. 8(b).

The magnetic viscosity $S(T)$ can be extracted from the relaxation data. In Fig. 9, we plot the magnetic viscosity $S(T)$ versus temperature for different applied fields H_2 ($=-1$, -4, -7, and -8 kOe). Here, it should be noted that the magnetic viscosity was measured from the whole sample, but some of the particles in the sample did not contribute to the relaxation depending on the applied field.

At temperatures $T \ll T_B$, the relaxation follows the logarithmic law:[1] when $T \sim T_B$, the relaxation will lose the logarithmic dependence because most of the particles have their relaxation times near or below that of the measuring time. For the applied field $H_2=-7$ and -8 kOe, the relaxation follows well the logarithmic time law in the temperature range 1.8–20 K (the experimental temperature range). For

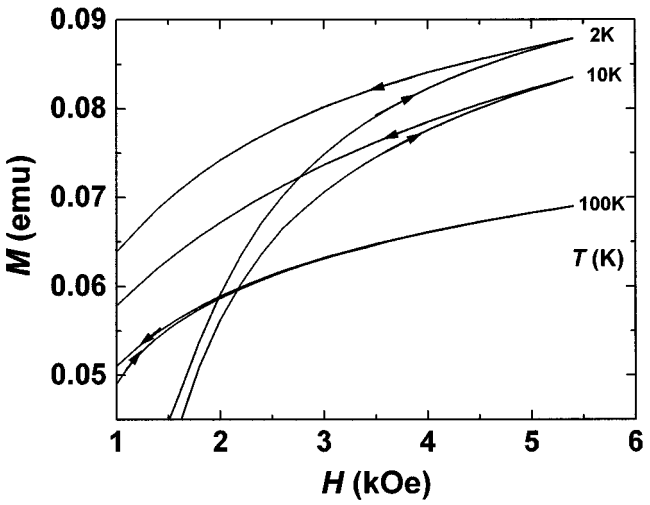

FIG. 5. Parts of hysterese loops obtained at different temperatures to show the irreversible field.

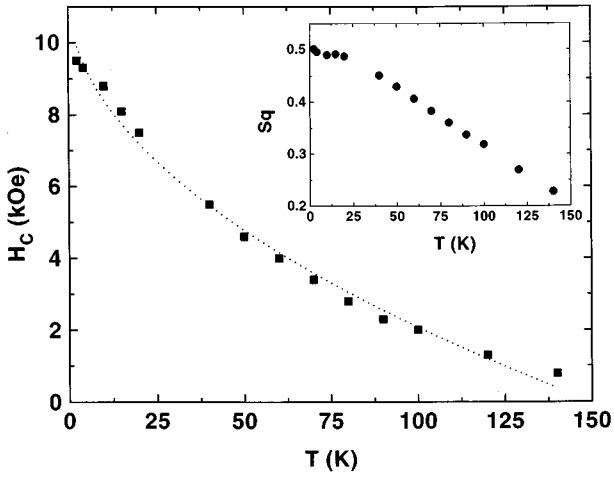

FIG. 7. Temperature dependence of coercive field H_C. Points: experimental. Line: fitting with a function $H_C(T)=H_C(0)[1-(T/T_B)^{1/2}]$. Inset: the temperature dependence of squareness $\mathrm{Sq}=Mr(H=0)/Ms(H=50\ \mathrm{kOe})$.

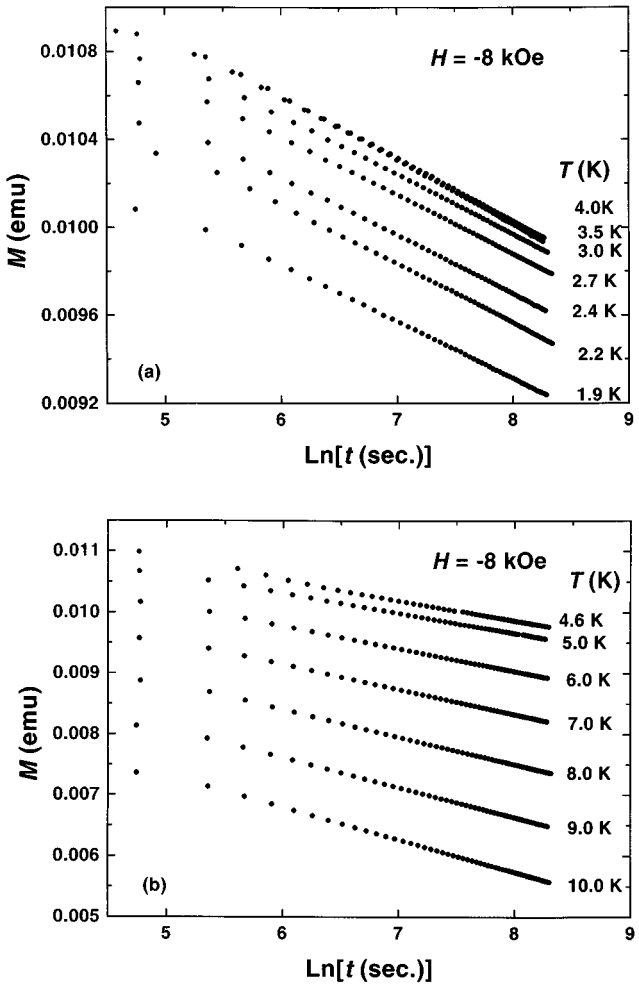

FIG. 8. Magnetization vs logarithm of time obtained in the relaxation measurements with applied field $H_2=-8$ kOe at different sample temperatures.

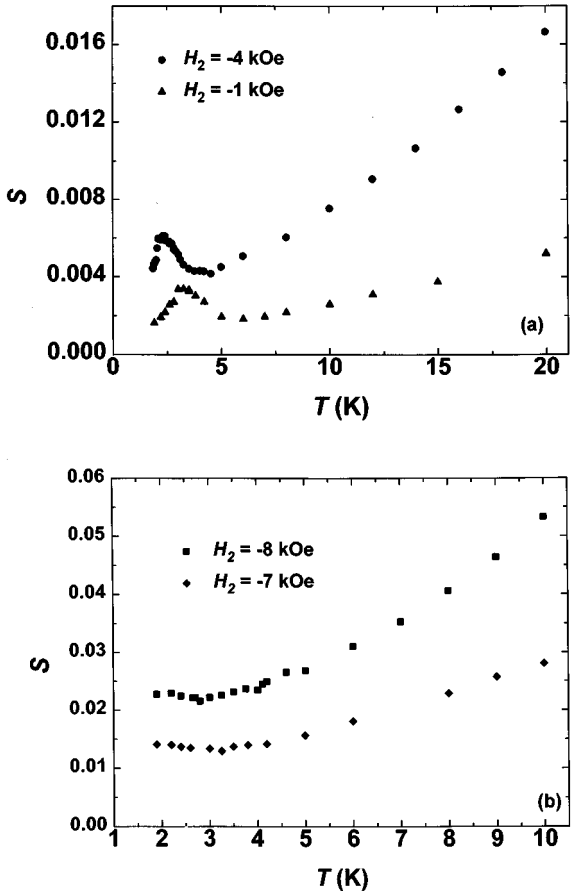

FIG. 9. Magnetic viscosity as a function of temperature obtained in the relaxation with applied field: (a) $H_2=-1$ and -4 kOe, (b) $H_2=-7$ and -8 kOe.

the lower applied field $H_2=-1$ and -4 kOe, the magnetic relaxation loses the logarithmic time dependence in the temperature range at which a peak appears in the viscosity curves (Fig. 9). The peaks which appear at the low-temperature range $T<5$ K in the $S(T)$ curves should be ascribed to the contribution of the particles in D_2. Figure 10 consists of two relaxation curves obtained with different applied field $H_2=-1$ and -8 kOe with sample temperatures of peak temperatures in the viscosity curves. For the applied field $H_2=-1$ kOe, there are peaks in the $S(T)$ curves, and the relaxation diverges from the logarithmic law, since most of the particles in D_2 are nearly unblocked. So the measured magnetic viscosity can be considered as the result of two origins, as we discussed the $M(H)$ curves: the particles in D_1 with blocking temperature $T_B>200$ K, and the particles in D_2 with blocking temperature $T_B\sim 6$ K. For $H_2=-8$ kOe, the relaxation follows very well the logarithmic time linear dependence, indicating that the particles in D_2 did not contribute to the relaxation, due to their superparamagnetic behavior in this applied field. This coincides with the fact that in the viscosity curve for $H_2=-7$ and -8 kOe, no peak was found in the temperature range $T<5$ K.

The most interesting feature in the behavior of the viscosity as a function of temperature shown in Fig. 9 is that all the viscosity data have a linear dependence on T in the high-temperature range from 5 to 20 K for applied field $H_2\leqslant 4$ kOe and $T>\sim 3$ K for $H_2\geqslant 7$ kOe, respectively, which corresponds to the thermally activated relaxation of the magnetization. As T goes to zero, the viscosity begins to be temperature independent at $T\sim 3$ K for $H=-7$ and -8 kOe; see Fig. 9(b). This temperature independence of the viscosity

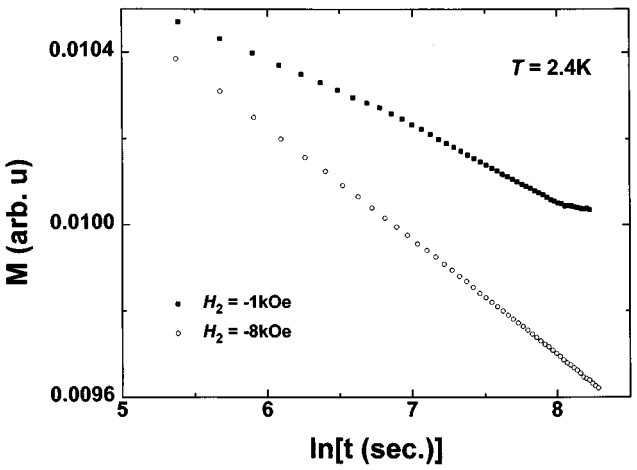

FIG. 10. Magnetic relaxation curve obtained with different applied field. $H_2=-1$ and -8 kOe.

is the signature of quantum tunneling of magnetization (QTM), as predicted theoretically.[1] It has been predicted theoretically that the crossover temperature from the thermal regime to the quantum tunneling regime scales with the magnetic anisotropy and also depends on the applied magnetic field in the relaxation measurements,[1,14] usually given by

$$k_B T_C \approx \mu_B H_K \varepsilon^{1/2}, \qquad \varepsilon = 1 - \frac{H}{H_K}, \tag{4}$$

where H_K is the anisotropy field of the materials. Thus tunneling should be observable at experimentally accessible temperature only for materials with high anisotropy, say $H_K \sim$T, with the relation T_C(K)$\sim H_K$(T). From the minimum of the anisotropy field which corresponds to the irreversible field in the hysteresis loops (Fig. 5), it is can be estimated, using Eq. (4), that the crossover temperature is $T_C \sim 5$ K for relaxations with a small applied field H_2. This is in correspondence with what was found in viscosity data, Fig. 9. With increasing applied field in the relaxation measurements, the crossover temperature T_C should be reduced, as predicted in Eq. (4).

The tunneling effect beginning at $\sim$3 K for $H > 4$ kOe should be considered as due only to the particles in D_1, because, as discussed above, at $T \geqslant 5$ K most of the particles in D_2 were in the superparamagnetic state, and did not contribute to the relaxation effect. For the applied field $H \leqslant 4$ kOe in the relaxation measurement, as temperature T goes to zero, the viscosity begins to increase and reaches a peak at $T \sim 3$ and 2.4 K for $H = 1$ and 4 kOe, respectively [Fig. 9(a)], and then decreases again, which appears to be contrary to the signature of QTM, temperature-independent viscosity at low-temperature regimes. One should remember, however, that with the applied field $H_2 = -1$ and -4 kOe, at the temperature range 1.8–5 K, some particles in D_2 are in the blocked state, and do contribute to relaxation. So the measured magnetic viscosity S for $-H_2 \leqslant 4$ kOe can be considered the sum of the quantum viscosity due to particles in D_1 and $S_{Q,D1}$ and the thermally activated magnetic viscosity, $S_{T,D2}$, i.e., $S = S_{Q,D1} + S_{T,D2}$, here $S_{Q,D1} \approx S(T = T_C \sim 5$ K). When the applied magnetic field $H_a = 7$ and 8 kOe in the relaxation measurements, the particles in D_2 behaved superparamagnetically, and did not contribute to the relaxation, $S_{T,D2} \sim 0$. As stated above, a purely temperature-independent viscosity of the sample, below the crossover temperature T_C, should be obtained which corresponds to the QTM of particles in D_1. This purely temperature-independent S below 3 K was observed clearly in the relaxation measurements with $H_2 = -7$ and -8 kOe; see Fig. 9(b).

In conclusion, we have studied the static and dynamic properties of a mixture of $CoFe_2O_4$ nanoparticles and a small quantity of γ-Fe_2O_3 nanoparticles with the same average diameter of 30 Å, in a wide range of temperature and applied magnetic field. The sample shows a very high effective anisotropy, the anisotropy field $H_K \sim 5$ T at 2.4 K. The high anisotropy leads to a high crossover temperature from the thermally activated regime to the quantum tunneling regime, $T_C \sim 5$ K in the applied fields, $-H_2 \leqslant 4$ kOe, and $T_C \sim 3$ K, with $H_2 = -7$ and -8 kOe, in coincidence with theoretical predictions. We also demonstrated experimentally that the energy distribution cannot give a temperature-independent viscosity. The energy distribution can be modified by applied magnetic field in the relaxation measurement; thus the singular energy distribution which is assumed to give a plateau in the viscosity $S(T)$ as function of temperature can be removed by the field.

ACKNOWLEDGMENTS

X.X.Z. acknowledges the financial support from the CIRIT de la Generalitat de Catalunya; J.M.H. acknowledges the financial support from Ministerio de Educación y Ciencia de España; J.T. the financial support from CICYT and European Community Project No. ERB4050PL930639.

*Author to whom correspondence should be addressed. Electronic address: xxz@hermes.ffn.ub.es

[1] J. Tejada, X. X. Zhang, and E. M. Chudnovsky, Phys. Rev. B **47**, 14 977 (1993).
[2] J. Tejada, X. X. Zhang, and L. Balcelles, J. Appl. Phys. **73**, 6709 (1993); J. Tejada and X. X. Zhang, J. Magn. Magn. Mater. **140–144**, 1815 (1995).
[3] B. Barbara *et al.*, J. Appl. Phys. **73**, 6703 (1993).
[4] R. H. Kodama, C. L. Seaman, A. E. Berkowitz, and M. B. Maple, J. Appl. Phys. **75**, 5639 (1994).
[5] X. X. Zhang, A. Garcia, J. Tejada, Y. Xin, and K. W. Wong, Physica C **232**, 99 (1994); A. Garcia, X. X. Zhang, J. Tejada, M. Manzel, and H. Gruchlos, Phys. Rev. B **50**, 9439 (1994); A. C. Mota *et al.*, *ibid*. **36**, 4011 (1987).
[6] X. X. Zhang, J. Tejada, A. Roig, O. Nikolov, and E. Molins, J. Magn. Magn. Mater. **137**, L235 (1994).
[7] C. Paulsen, J. G. Park, B. Barbara, R. Sessoli, and A. Caneshi, J. Magn. Magn. Mater. **140–144**, 1891 (1995).
[8] J. R. Friedman, M. P. Sarachik, J. Tejada, and R. F. Ziolo, Phys. Rev. Lett. **76**, 3830 (1996); J. M. Hernández, X. X. Zhang, J. Tejada, J. R. Friedman, M. P. Sarachik, and R. F. Ziolo (unpublished).
[9] B. Barbara and L. Gunther, J. Magn. Magn. Mater. **128**, 35 (1993).
[10] R. F. Ziolo *et al.*, Science **257**, 219 (1992).
[11] R. F. Ziolo (unpublished).
[12] E. F. Kneller and F. E. Luborsky, J. Appl. Phys. **34**, 656 (1963).
[13] C. P. Bean and J. D. Limingston, J. Appl. Phys. **30**, 120S (1959).
[14] E. M. Chudnovsky and L. Gunther, Phys. Rev. Lett. **60**, 661 (1988); Phys. Rev. B **37**, 9455 (1988).